Electronic Supplementary Information (ESI)

An efficient and robust procedure to calculate absorption spectra of aqueous charged species applied to NO_2^-

Lina Uribe,[†] Sara Gómez,[‡] Tommaso Giovannini,[‡] Franco Egidi,[‡] and Albeiro Restrepo[†]

[†]*Instituto de Química, Universidad de Antioquia UdeA, Calle 70 No. 52-21, Medellín, Colombia*
[‡]*Scuola Normale Superiore, Classe di Scienze, Piazza dei Cavalieri 7, 56126, Pisa, Italy*

*Correspondence: sara.gomezmaya@sns.it, albeiro.restrepo@udea.edu.co

Contents

1 MD simulations

Table S1: Conditions for the MD simulations of the NO_2^- in aqueous solution

Item	Description
MD package	GROMACS 2020.3[1]
Solute charges	CM5[2] and RESP[3]
Force field	GAFF[4]
Water molecules	TIP3P[5]
Energy minimization	steepest descent minimization algorithm
NVT equilibration	total time: 0.2 ns velocity-rescaling method[6] integration time step: 0.2 fs coupling constant: 0.1 ps
NPT equilibration	total time: 1 ns integration time step: 1 fs barostat: Parrinello–Rahman[7]
NPT production	total time: 50 ns integration time step: 2 fs LINCS algorithm Electrostatic interactions: Particle Mesh Ewald (PME)[8] grid spacing: 0.16 nm cubic interpolation Coulomb cut-off: 1.0 nm leap-frog algorithm[9]

2 ASCEC conditions

Table S2: Specific annealing conditions used in the exploration of the PES of $[NO_2\,(H_2O)_x]^-$ clusters with $x = 1 - 6$. To eliminate structural bias, all ASCEC runs used the big bang initial conditions, that is, all individual molecules were superimposed at the center of the cubic box and the system was allowed to evolve under the annealing conditions.

Parameter	x					
	1	**2**	**3**	**4**	**5**	**6**
Cube's length (Å)	3	5	8	10	10	12
Number of replicas	2	2	2	2	3	4
MaxCycle	1000	1000	1000	1000	3000	3000
Quenching route	T_0=600 K, %dism=10, 200 steps					
Method	B3LYP					
Basis set	6–31g(d)					

3 Radial distribution functions

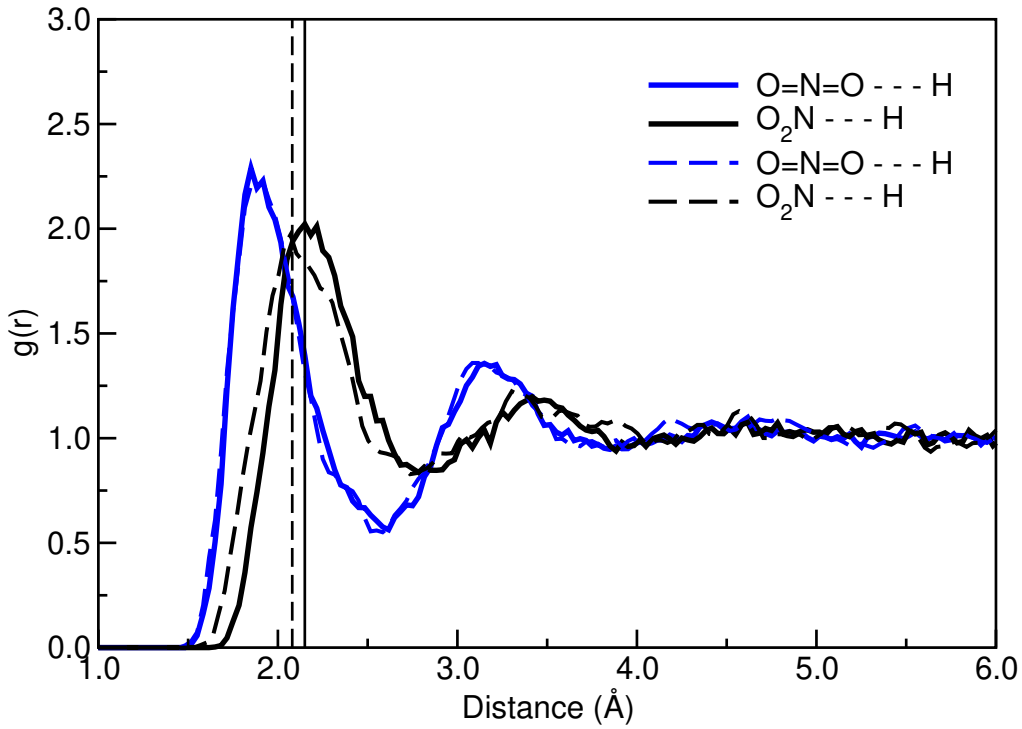

Figure S1: Radial distribution functions (RDFs) between Oxygen atoms of NO_2^- and water Hydrogen atoms, as obtained from MD with CM5 charges (solid lines) and MD with RESP charges (dashed line) runs

4 Energies and isomer populations

Table S3: Binding energies in kcal/mol and isomer populations ($\%\chi_i$) derived from Boltzmann distributions of the isomer energies for the entire set of structures derived from ASCEC. All quantities calculated using the ZPE–corrected electronic (E), Enthalpy (H) and Gibbs (G) potential energy surfaces at room conditions.

Structures	$-$BE	$-$BE$_H$	$-$BE$_G$	$\%\chi_i$E	$\%\chi_i$H	$\%\chi_i$G
W_1S_1	16.13	16.72	8.01	89.51	90.52	85.30
W_1S_2	14.69	15.24	6.65	7.95	7.40	8.60
W_1S_3	13.71	14.08	6.32	1.51	1.04	4.95
W_1S_4	13.49	14.08	5.46	1.04	1.04	1.15
W_2S_1	28.57	29.49	12.64	66.87	53.00	74.90
W_2S_2	27.30	28.44	11.39	7.88	8.93	9.15
W_2S_3	26.60	27.34	11.36	2.39	1.41	8.59
W_2S_4	27.65	29.00	10.89	14.19	23.32	3.92
W_2S_5	26.83	28.05	10.19	3.55	4.67	1.19
W_2S_6	25.69	26.79	9.98	0.52	0.55	0.83
W_2S_7	25.88	27.02	9.71	0.52	0.55	0.83
W_2S_8	26.73	28.17	9.48	2.98	5.70	0.36
W_2S_9	25.30	27.39	8.92	0.87	1.54	0.14
W_3S_1	38.59	39.94	15.16	7.58	4.04	27.90
W_3S_2	38.75	40.15	15.11	9.89	5.83	25.39
W_3S_3	38.44	39.82	15.04	5.91	3.32	22.57
W_3S_4	38.53	40.09	14.22	6.77	5.26	5.67
W_3S_5	38.90	40.56	14.17	12.86	11.47	5.25
W_3S_6	39.28	41.00	14.13	24.04	24.29	4.90
W_3S_7	38.01	39.50	13.63	2.83	1.94	2.08
W_3S_8	38.52	40.21	13.50	6.72	6.38	1.68
W_3S_9	38.41	40.27	13.22	5.58	7.07	1.05
W_3S_{10}	36.51	38.15	13.02	0.23	0.20	0.74
W_3S_{11}	37.94	39.76	12.92	2.51	2.99	0.63
W_3S_{12}	38.05	40.03	12.62	3.05	4.75	0.38
W_3S_{13}	36.61	38.14	12.51	0.27	0.20	0.32
W_3S_{14}	37.77	39.72	12.21	1.90	2.79	0.19
W_3S_{15}	35.75	37.36	12.14	0.06	0.05	0.17
W_3S_{16}	37.41	39.33	12.03	1.04	1.46	0.14
W_3S_{17}	35.70	37.13	12.02	0.06	0.04	0.14
W_3S_{18}	36.91	38.82	11.91	0.44	0.62	0.12
W_3S_{19}	34.78	36.28	11.72	0.01	0.01	0.08
W_3S_{20}	37.61	39.65	11.71	1.44	2.48	0.08
W_3S_{21}	36.42	38.25	11.69	0.19	0.23	0.08
W_3S_{22}	37.31	39.30	11.69	0.87	1.37	0.08

W_3S_{23}	36.63	38.49	11.68	0.28	0.35	0.08
W_3S_{24}	38.26	40.54	11.59	4.32	11.15	0.07
W_3S_{25}	34.87	36.48	11.54	0.01	0.01	0.06
W_3S_{26}	37.27	39.25	11.47	0.81	1.26	0.06
W_3S_{27}	34.61	36.20	11.45	0.01	0.01	0.05
W_3S_{28}	36.56	38.44	11.26	0.25	0.32	0.04
W_3S_{29}	35.03	36.59	10.47	0.02	0.01	0.01
W_3S_{30}	35.83	37.77	10.23	0.07	0.11	0.01
W_4S_1	48.50	49.96	17.75	5.49	1.42	46.46
W_4S_2	48.24	49.75	17.34	3.54	0.99	23.44
W_4S_3	48.85	50.91	16.51	10.02	7.05	5.76
W_4S_4	48.77	50.88	16.12	8.66	6.74	2.97
W_4S_5	46.80	48.50	16.10	0.31	0.12	2.91
W_4S_6	48.35	50.41	16.07	4.29	3.00	2.77
W_4S_7	48.12	49.90	16.05	2.89	1.27	2.67
W_4S_8	48.83	50.99	15.94	9.56	8.12	2.22
W_4S_9	48.75	50.91	15.90	8.45	6.99	2.05
W_4S_{10}	48.11	50.19	15.83	2.85	2.09	1.84
W_4S_{11}	48.16	50.25	15.53	3.11	2.30	1.10
W_4S_{12}	48.23	50.36	15.44	3.48	2.79	0.95
W_4S_{13}	48.21	50.32	15.44	3.37	2.61	0.95
W_4S_{14}	47.14	49.09	15.27	0.56	0.33	0.71
W_4S_{15}	47.08	49.27	15.10	0.50	0.45	0.54
W_4S_{16}	47.31	49.66	15.10	0.74	0.85	0.54
W_4S_{17}	47.34	49.33	14.75	0.77	0.49	0.29
W_4S_{18}	48.55	50.96	14.65	6.03	7.66	0.25
W_4S_{19}	47.37	49.48	14.60	0.82	0.63	0.23
W_4S_{20}	46.76	48.77	14.53	0.29	0.19	0.20
W_4S_{21}	46.65	48.62	14.44	0.24	0.15	0.18
W_4S_{22}	47.82	49.90	14.37	1.75	1.27	0.16
W_4S_{23}	46.52	48.51	14.24	0.20	0.12	0.13
W_4S_{24}	48.87	50.31	14.17	1.92	2.58	0.11
W_4S_{25}	46.32	48.30	14.14	0.14	0.09	0.11
W_4S_{26}	46.31	48.30	14.13	0.14	0.09	0.10
W_4S_{27}	47.38	49.87	13.97	0.83	1.22	0.08
W_4S_{28}	48.25	50.82	13.91	3.62	6.05	0.07
W_4S_{29}	48.24	50.76	13.65	3.53	5.45	0.05
W_4S_{30}	47.43	49.65	13.58	0.91	0.85	0.04
W_4S_{31}	48.43	51.32	13.58	4.93	14.02	0.04
W_4S_{32}	47.50	49.99	13.34	1.02	1.49	0.03
W_4S_{33}	45.62	48.03	13.07	0.04	0.06	0.02
W_4S_{34}	47.42	50.02	13.04	0.89	1.57	0.02

W_4S_{35}	47.53	50.16	12.74	1.07	2.00	0.01
W_4S_{36}	47.44	50.07	12.71	0.92	1.70	0.01
W_4S_{37}	46.46	49.06	12.61	0.18	0.31	0.01
W_4S_{38}	45.25	47.56	12.59	0.02	0.03	0.01
W_4S_{39}	45.36	47.72	12.58	0.03	0.03	0.01
W_4S_{40}	42.67	44.64	12.32	0.00	0.00	0.01
W_4S_{41}	47.10	49.91	12.32	0.52	1.29	0.01
W_4S_{42}	47.33	50.10	12.29	0.77	1.80	0.01
W_4S_{43}	46.56	49.18	12.26	0.21	0.38	0.00
W_4S_{44}	45.70	48.37	11.48	0.05	0.10	0.00
W_4S_{45}	46.09	48.87	11.31	0.09	0.22	0.00
W_4S_{46}	45.75	48.41	11.29	0.05	0.10	0.00
W_4S_{47}	46.62	49.73	10.73	0.23	0.96	0.00
W_4S_{48}	44.31	46.64	10.58	0.01	0.01	0.00
W_5S_1	57.05	58.83	18.92	0.69	0.04	34.97
W_5S_2	57.20	59.08	18.90	0.88	0.05	33.73
W_5S_3	56.87	58.75	18.41	0.51	0.03	14.84
W_5S_4	57.53	59.71	17.86	1.54	0.16	5.85
W_5S_5	57.94	60.52	17.32	3.09	0.62	2.37
W_5S_6	58.19	60.95	17.07	4.73	1.28	1.55
W_5S_7	56.78	59.03	16.95	0.43	0.05	1.25
W_5S_8	56.07	58.41	16.91	0.13	0.02	1.17
W_5S_9	58.36	61.19	16.66	6.30	1.90	0.78
W_5S_{10}	57.06	59.91	16.40	0.70	0.22	0.50
W_5S_{11}	58.40	61.38	16.37	6.72	2.64	0.47
W_5S_{12}	57.13	59.58	16.31	0.79	0.13	0.43
W_5S_{13}	56.26	58.79	16.03	0.18	0.03	0.27
W_5S_{14}	57.04	60.00	16.01	0.68	0.25	0.26
W_5S_{15}	55.92	58.44	15.90	0.10	0.02	0.22
W_5S_{16}	55.52	58.22	15.88	0.05	0.01	0.21
W_5S_{17}	56.86	59.59	15.57	0.50	0.13	0.12
W_5S_{18}	57.99	60.75	15.51	3.35	0.91	0.11
W_5S_{19}	56.96	59.75	15.46	0.59	0.17	0.10
W_5S_{20}	58.51	61.74	15.42	8.04	4.86	0.10
W_5S_{21}	56.98	59.56	15.35	0.61	0.12	0.08
W_5S_{22}	57.72	60.81	15.23	2.11	1.01	0.07
W_5S_{23}	57.53	60.59	15.23	1.55	0.69	0.07
W_5S_{24}	55.61	58.21	15.22	0.06	0.01	0.07
W_5S_{25}	57.53	60.59	15..02	1.56	0.70	0.05
W_5S_{26}	56.98	59.83	14.99	0.61	0.19	0.05
W_5S_{27}	56.58	59.21	14.88	0.31	0.07	0.04
W_5S_{28}	57.37	60.31	14.84	1.18	0.43	0.04

W_5S_{29}	55.39	57.92	14.65	0.04	0.01	0.03
W_5S_{30}	58.13	61.58	14.61	4.24	3.69	0.02
W_5S_{31}	57.43	60.84	14.58	1.29	1.06	0.02
W_5S_{32}	54.80	57.23	14.58	0.02	0.00	0.02
W_5S_{33}	57.54	60.76	14.58	1.57	0.92	0.02
W_5S_{34}	56.63	59.68	14.53	0.34	0.15	0.02
W_5S_{35}	56.54	59.37	14.45	0.29	0.09	0.02
W_5S_{36}	53.60	55.94	14.20	0.00	0.00	0.01
W_5S_{37}	55.84	58.85	14.14	0.09	0.04	0.01
W_5S_{38}	56.76	60.06	14.13	0.42	0.28	0.01
W_5S_{39}	56.58	59.49	14.11	0.31	0.11	0.01
W_5S_{40}	52.93	55.33	14.06	0.00	0.00	0.01
W_5S_{41}	54.06	56.49	13.89	0.00	0.00	0.01
W_5S_{42}	53.95	56.56	13.88	0.00	0.00	0.01
W_5S_{43}	59.44	63.35	13.80	39.15	72.56	0.01
W_5S_{44}	57.58	60.88	13.69	1.68	1.13	0.01
W_5S_{45}	55.67	58.62	13.69	0.07	0.03	0.01
W_5S_{46}	55.49	58.58	13.62	0.05	0.02	0.01
W_5S_{47}	55.25	58.13	13.24	0.03	0.01	0.00
W_5S_{48}	54.72	57.29	13.20	0.01	0.00	0.00
W_5S_{49}	56.75	60.21	12.93	0.41	0.37	0.00
W_5S_{50}	55.61	59.00	12.92	0.06	0.05	0.00
W_5S_{51}	55.75	59.14	12.88	0.08	0.06	0.00
W_5S_{52}	55.45	58.55	12.85	0.05	0.02	0.00
W_5S_{53}	56.35	59.82	12.75	0.21	0.19	0.00
W_5S_{54}	53.95	56.86	12.40	0.00	0.00	0.00
W_5S_{55}	55.98	59.53	12.28	0.11	0.12	0.00
W_5S_{56}	54.45	57.57	12.25	0.01	0.00	0.00
W_5S_{57}	57.41	61.25	12.21	1.26	2.13	0.00
W_5S_{58}	56.06	59.64	12.01	0.13	0.14	0.00
W_5S_{59}	54.90	58.05	11.87	0.02	0.01	0.00
W_5S_{60}	54.99	58.41	11.80	0.02	0.02	0.00
W_5S_{61}	55.06	58.67	11.67	0.02	0.03	0.00
W_5S_{62}	53.18	56.28	11.03	0.00	0.00	0.00
W_5S_{63}	53.12	56.09	10.97	0.00	0.00	0.00
W_5S_{64}	54.90	58.61	10.78	0.02	0.02	0.00
W_5S_{65}	53.43	57.11	9.13	0.00	0.00	0.00
W_5S_{66}	52.49	56.23	8.87	0.00	0.00	0.00
W_5S_{67}	49.09	52.28	8.34	0.00	0.00	0.00
W_5S_{68}	51.35	54.54	8.18	0.00	0.00	0.00
W_6S_1	65.30	67.33	20.28	0.12	0.00	56.99
W_6S_2	65.15	67.33	19.38	0.10	0.00	12.49

W_6S_3	64.65	67.30	19.37	0.04	0.00	12.26
W_6S_4	64.47	66.63	18.87	0.03	0.00	5.27
W_6S_5	64.95	67.52	18.71	0.07	0.00	4.08
W_6S_6	65.61	68.55	18.47	0.21	0.02	2.68
W_6S_7	64.42	66.81	18.43	0.03	0.00	2.51
W_6S_8	67.00	68.66	17.97	0.41	0.02	1.17
W_6S_9	64.89	67.44	17.39	0.06	0.00	0.44
W_6S_{10}	66.40	69.70	16.92	0.79	0.11	0.21
W_6S_{11}	67.05	70.41	16.96	2.41	0.36	0.21
W_6S_{12}	63.84	66.62	16.88	0.01	0.00	0.18
W_6S_{13}	66.54	69.66	16.86	1.01	0.10	0.18
W_6S_{14}	65.54	68.57	16.77	0.19	0.02	0.15
W_6S_{15}	66.07	69.39	16.70	0.46	0.06	0.14
W_6S_{16}	64.17	67.19	16.41	0.02	0.00	0.08
W_6S_{17}	64.55	67.35	16.38	0.04	0.00	0.08
W_6S_{18}	66.51	69.80	16.38	0.96	0.13	0.08
W_6S_{19}	64.23	66.98	16.34	0.02	0.00	0.08
W_6S_{20}	64.76	67.76	16.3	0.05	0.00	0.07
W_6S_{21}	65.64	68.64	16.30	0.22	0.02	0.07
W_6S_{22}	65.89	69.17	16.23	0.34	0.04	0.06
W_6S_{23}	64.18	66.79	16.20	0.02	0.00	0.06
W_6S_{24}	65.69	68.78	16.12	0.24	0.02	0.05
W_6S_{25}	62.97	65.71	16.07	0.00	0.00	0.05
W_6S_{26}	64.00	67.06	15.93	0.01	0.00	0.04
W_6S_{27}	63.39	66.32	15.69	0.01	0.00	0.03
W_6S_{28}	63.51	66.48	15.68	0.01	0.00	0.02
W_6S_{29}	65.01	68.15	15.67	0.08	0.01	0.02
W_6S_{30}	63.74	67.12	15.58	0.01	0.00	0.02
W_6S_{31}	64.98	68.14	15.50	0.07	0.01	0.02
W_6S_{32}	65.97	69.45	15.49	0.39	0.07	0.02
W_6S_{33}	64.71	67.76	15.41	0.05	0.00	0.02
W_6S_{34}	62.70	65.29	15.39	0.00	0.00	0.02
W_6S_{35}	65.59	68.94	15.31	0.21	0.03	0.01
W_6S_{36}	66.22	69.63	15.28	0.59	0.10	0.01
W_6S_{37}	62.46	65.66	15.21	0.00	0.00	0.01
W_6S_{38}	64.63	67.54	15.17	0.04	0.00	0.01
W_6S_{39}	66.81	70.72	15.14	1.61	0.6	0.01
W_6S_{40}	65.98	69.46	15.10	0.39	0.07	0.01
W_6S_{41}	63.90	67.07	15.07	0.01	0.00	0.01
W_6S_{42}	64.92	68.24	15.07	0.07	0.01	0.01
W_6S_{43}	66.24	70.16	15.07	0.61	0.23	0.01
W_6S_{44}	63.37	66.21	14.93	0.01	0.00	0.01

W_6S_{45}	64.54	68.07	14.90	0.04	0.01	0.01
W_6S_{46}	62.45	65.29	14.90	0.00	0.00	0.01
W_6S_{47}	66.19	69.78	14.88	0.56	0.12	0.01
W_6S_{48}	65.99	69.64	14.87	0.40	0.10	0.01
W_6S_{49}	65.53	69.32	14.65	0.18	0.06	0.00
W_6S_{50}	69.12	73.70	14.65	78.73	90.76	0.00
W_6S_{51}	64.30	67.68	14.63	0.03	0.00	0.00
W_6S_{52}	62.62	65.62	14.57	0.00	0.00	0.00
W_6S_{53}	62.94	66.13	14.51	0.00	0.00	0.00
W_6S_{54}	63.31	66.81	14.41	0.00	0.00	0.00
W_6S_{55}	66.81	70.88	14.41	1.61	0.78	0.00
W_6S_{56}	64.95	68.52	14.23	0.07	0.02	0.00
W_6S_{57}	64.86	68.30	14.15	0.06	0.01	0.00
W_6S_{58}	64.61	68.17	14.05	0.04	0.01	0.00
W_6S_{59}	65.92	70.01	14.04	0.36	0.18	0.00
W_6S_{60}	64.89	68.33	13.96	0.06	0.01	0.00
W_6S_{61}	62.98	66.11	13.93	0.00	0.00	0.00
W_6S_{62}	66.52	70.99	13.85	0.99	0.95	0.00
W_6S_{63}	65.05	68.88	13.84	0.08	0.03	0.00
W_6S_{64}	65.67	69.60	13.71	0.23	0.09	0.00
W_6S_{65}	64.52	68.06	13.68	0.03	0.06	0.00
W_6S_{66}	63.87	67.34	13.60	0.01	0.00	0.00
W_6S_{67}	64.16	68.02	13.57	0.02	0.00	0.00
W_6S_{68}	59.88	62.57	13.33	0.00	0.00	0.00
W_6S_{69}	62.23	65.49	13.27	0.00	0.00	0.00
W_6S_{70}	63.35	66.82	13.26	0.00	0.00	0.00
W_6S_{71}	65.39	69.52	13.25	0.14	0.08	0.00
W_6S_{72}	66.43	70.91	13.20	0.83	0.82	0.00
W_6S_{73}	65.12	69.08	13.17	0.09	0.04	0.00
W_6S_{74}	64.77	68.49	13.14	0.05	0.01	0.00
W_6S_{75}	63.82	67.49	13.07	0.01	0.00	0.00
W_6S_{76}	63.30	66.82	13.06	0.00	0.00	0.00
W_6S_{77}	61.51	64.47	13.03	0.00	0.00	0.00
W_6S_{78}	63.25	67.00	12.99	0.00	0.00	0.00
W_6S_{79}	64.89	69.00	12.95	0.06	0.03	0.00
W_6S_{80}	63.79	67.52	12.92	0.01	0.00	0.00
W_6S_{81}	65.37	69.39	12.83	0.14	0.06	0.00
W_6S_{82}	60.71	63.34	12.83	0.00	0.00	0.00
W_6S_{83}	64.26	68.09	12.74	0.02	0.01	0.00
W_6S_{84}	63.07	66.62	12.69	0.00	0.00	0.00
W_6S_{85}	65.53	69.57	12.62	0.18	0.09	0.00
W_6S_{86}	64.83	68.68	12.62	0.06	0.02	0.00

W_6S_{87}	64.16	68.20	12.44	0.02	0.01	0.00
W_6S_{88}	66.70	71.26	12.34	1.33	1.49	0.00
W_6S_{89}	66.43	71.22	12.14	0.84	1.40	0.00
W_6S_{90}	63.80	67.51	12.13	0.01	0.00	0.00
W_6S_{91}	64.10	68.09	12.06	0.02	0.00	0.00
W_6S_{92}	64.44	68.62	12.01	0.03	0.02	0.00
W_6S_{93}	65.73	70.03	11.93	0.26	0.19	0.00
W_6S_{94}	62.79	66.61	11.58	0.00	0.00	0.00
W_6S_{95}	63.55	67.47	11.54	0.01	0.00	0.00
W_6S_{96}	60.90	64.91	11.46	0.00	0.00	0.00
W_6S_{97}	62.23	65.84	11.40	0.00	0.00	0.00
W_6S_{98}	61.68	65.47	11.39	0.00	0.00	0.00
W_6S_{99}	61.981	65.55	11.30	0.00	0.00	0.00
W_6S_{100}	60.34	64.05	11.07	0.00	0.00	1.02
W_6S_{101}	65.56	70.12	11.00	0.19	0.22	0.00
W_6S_{102}	65.47	70.37	10.77	0.17	0.33	0.00
W_6S_{103}	60.54	64.28	10.26	0.00	0.00	0.00
W_6S_{104}	62.84	67.12	9.96	0.00	0.00	0.00
W_6S_{105}	62.22	66.45	9.90	0.00	0.00	0.00
W_6S_{106}	59.36	62.83	9.49	0.00	0.00	0.00
W_6S_{107}	61.69	65.71	9.23	0.00	0.00	0.00
W_6S_{108}	58.12	61.86	8.20	0.00	0.00	0.00
W_6S_{109}	57.68	61.60	6.14	0.00	0.00	0.00
W_6S_{110}	51.89	56.44	0.47	0.00	0.00	0.00

5 Structural motifs

PES for $[NO_2\,(H_2O)_x]^-$

5.1 $x = 1$

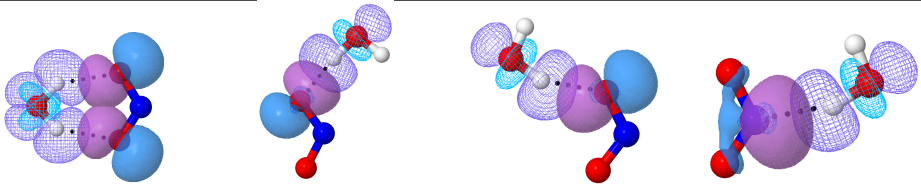

W_1S_1; ΔE_G=0.00 ΔE=0.00 | W_1S_2; ΔE_G=1.36 ΔE=1.43 | W_1S_3; ΔE_G=1.69 ΔE=2.42 | W_1S_4; ΔE_G=2.55 ΔE=2.64

Figure S2: Structural motifs on the potential energy surface for $[NO_2(H_2O)]^-$. Dotted lines correspond to intermolecular contacts, those for which AIM predicts bonding paths. Data taken from the B3LYP/6-311++G(d,p) optimized geometries.

5.2 $x = 2$

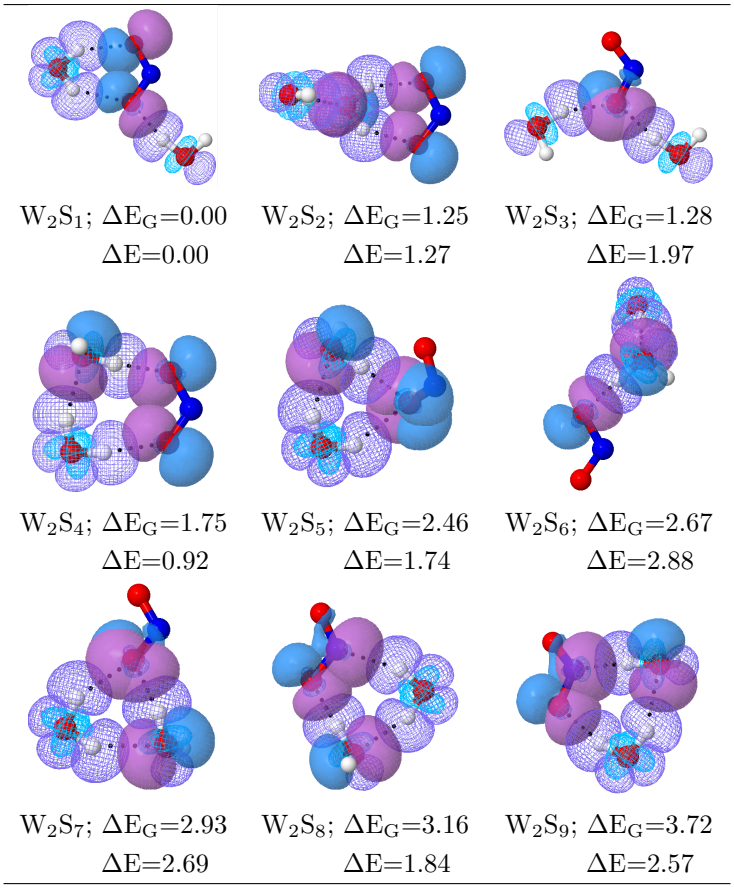

Figure S3: Structural motifs on the potential energy surface for $[NO_2(H_2O)_2]^-$. Dotted lines correspond to intermolecular contacts, those for which AIM predicts bonding paths. Data taken from the B3LYP/6-311++G(d,p) optimized geometries.

5.3 $x = 3$

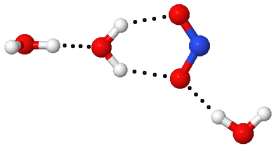

W_3S_1; ΔE_G=0.00
ΔE=0.68

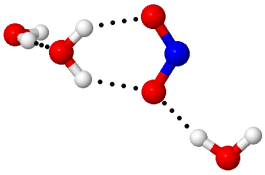

W_3S_2; ΔE_G=0.06
ΔE=0.53

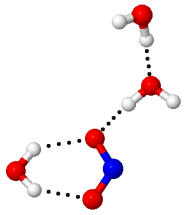

W_3S_3; ΔE_G=0.13
ΔE=0.83

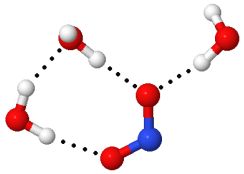

W_3S_4; ΔE_G=0.94
ΔE=0.75

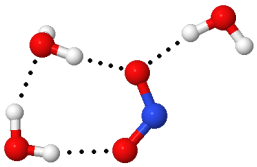

W_3S_5; ΔE_G=0.99
ΔE=0.37

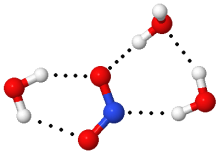

W_3S_6; ΔE_G=1.03
ΔE=0.00

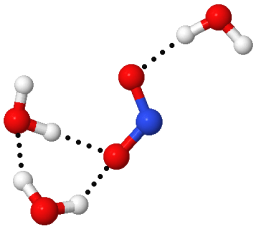

W_3S_7; ΔE_G=1.54
ΔE=1.27

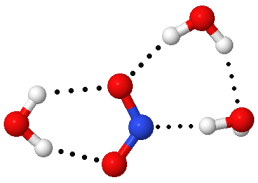

W_3S_8; ΔE_G=1.67
ΔE=0.75

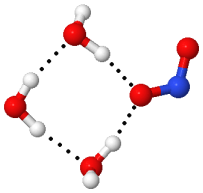

W_3S_9; ΔE_G=1.94
ΔE=0.87

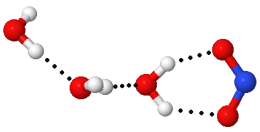

W_3S_{10}; ΔE_G=2.15
ΔE=2.77

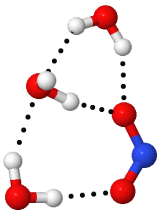

W_3S_{11}; ΔE_G=2.25
ΔE=1.34

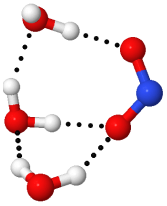

W_3S_{12}; ΔE_G=2.54
ΔE=1.22

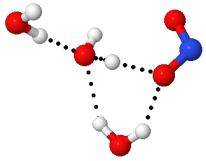

W_3S_{13}; ΔE_G=2.65
ΔE=2.67

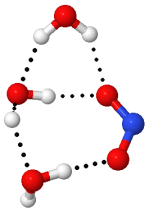

W_3S_{14}; ΔE_G=2.96
ΔE=1.51

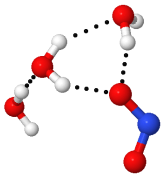

W_3S_{15}; ΔE_G=3.02
ΔE=3.52

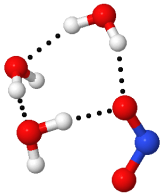

W_3S_{16}; ΔE_G=3.13
ΔE=1.86

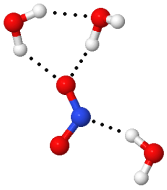

W_3S_{17}; ΔE_G=3.15
ΔE=3.58

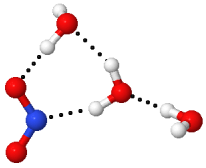

W_3S_{18}; ΔE_G=3.25
ΔE=2.37

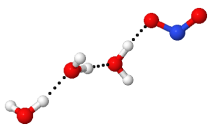

W_3S_{19}; ΔE_G=3.45
ΔE=4.50

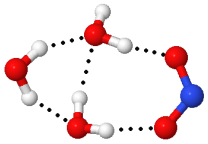

W_3S_{20}; ΔE_G=3.45
ΔE=1.67

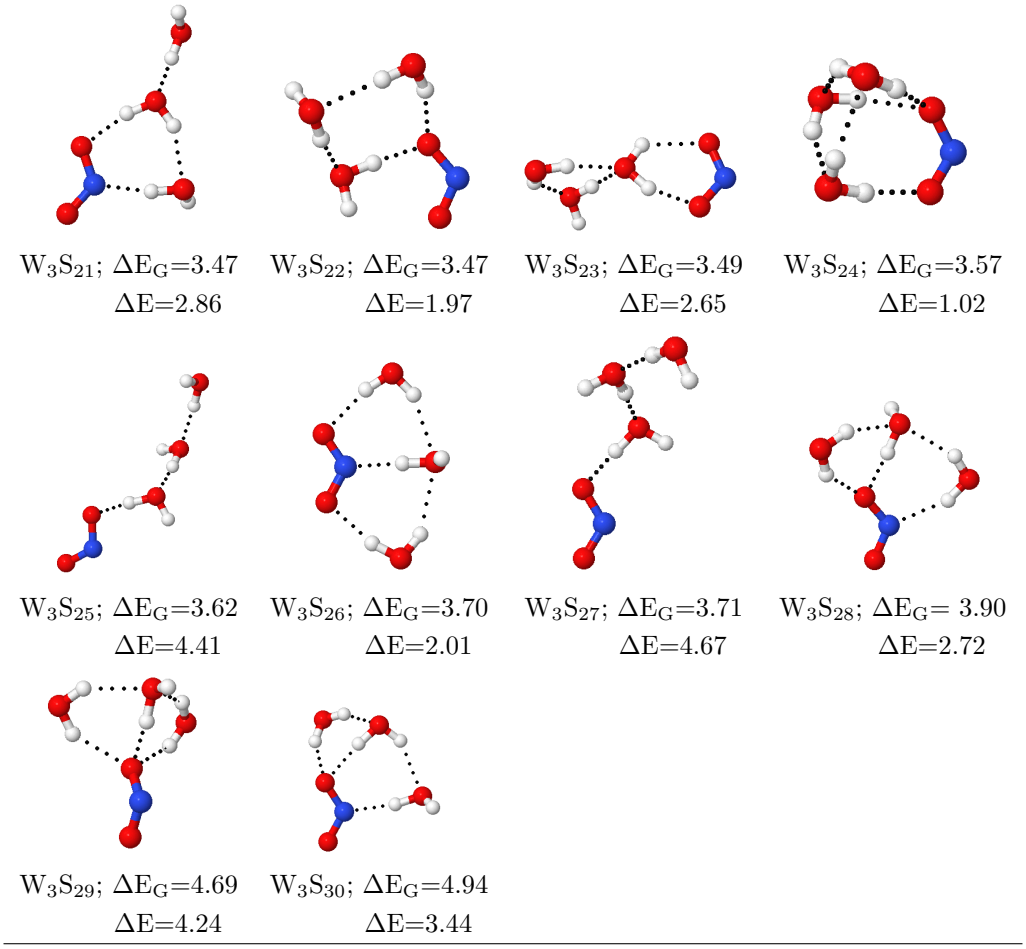

Figure S4: Structural motifs on the potential energy surface for $[NO_2(H_2O)_3]^-$. Dotted lines correspond to intermolecular contacts, those for which AIM predicts bonding paths. Data taken from the B3LYP/6-311++G(d,p) optimized geometries.

5.4 $x = 4$

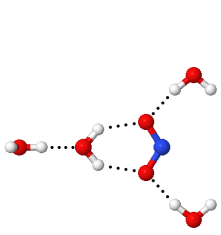

W_4S_1; ΔE_G=0.00
ΔE=0.36

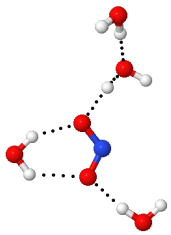

W_4S_2; ΔE_G=0.41
ΔE=0.62

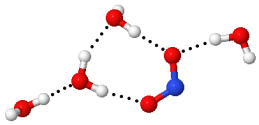

W_4S_3; ΔE_G=1.24
ΔE=0.00

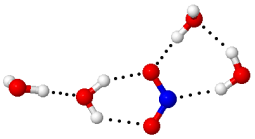

W_4S_4; ΔE_G=1.63
ΔE=0.09

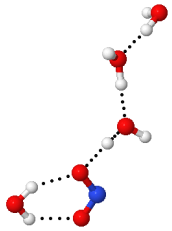

W_4S_5; ΔE_G=1.64
ΔE=2.06

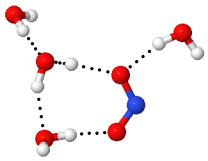

W_4S_6; ΔE_G=1.67
ΔE=0.50

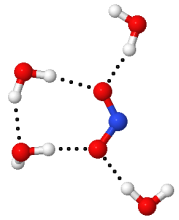

W_4S_7; ΔE_G=1.69
ΔE=0.74

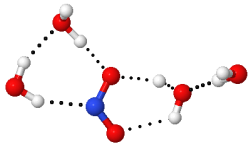

W_4S_8; ΔE_G=1.80
ΔE=0.03

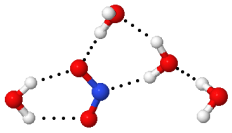

W_4S_9; ΔE_G=1.85
ΔE=0.10

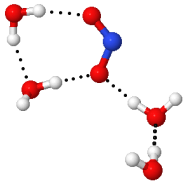

W_4S_{10}; ΔE_G=1.92
ΔE=0.75

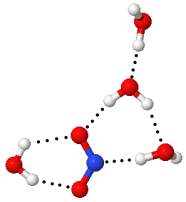

W_4S_{11}; ΔE_G=2.22
ΔE=0.69

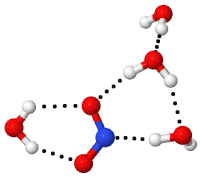

W_4S_{12}; ΔE_G=2.30
ΔE=0.63

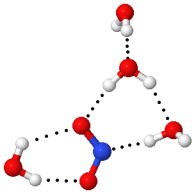

W_4S_{13}; ΔE_G=2.31
ΔE=0.65

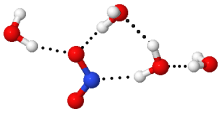

W_4S_{14}; ΔE_G=2.45
ΔE=1.71

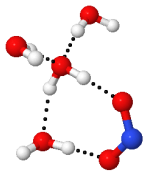

W_4S_{15}; ΔE_G=2.64
ΔE=1.78

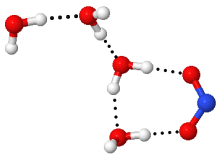

W_4S_{16}; ΔE_G=2.65
ΔE=1.54

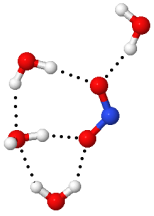

W_4S_{17}; ΔE_G=3.00
ΔE=1.52

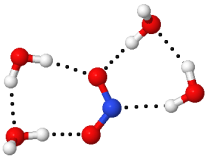

W_4S_{18}; ΔE_G=3.10
ΔE=0.30

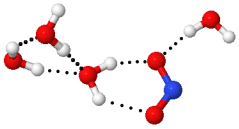

W_4S_{19}; ΔE_G=3.15
ΔE=1.48

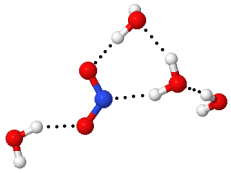

W_4S_{20}; ΔE_G= 3.22
ΔE=2.09

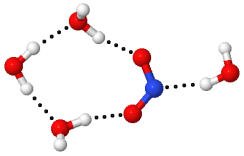

W_4S_{21}; ΔE_G=3.30
ΔE=2.20

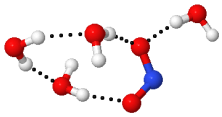

W_4S_{22}; ΔE_G=3.38
ΔE=1.03

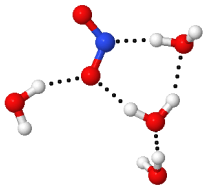

W_4S_{23}; ΔE_G=3.51
ΔE=2.33

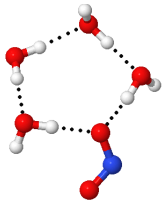

W_4S_{24}; ΔE_G=3.57
ΔE=0.98

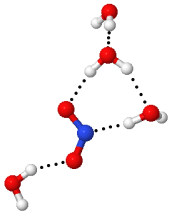

W_4S_{25}; ΔE_G=3.61
ΔE=2.54

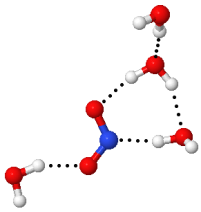

W_4S_{26}; ΔE_G=3.62
ΔE=2.54

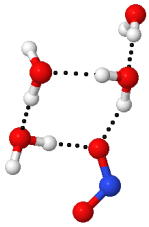

W_4S_{27}; ΔE_G=3.78
ΔE=1.48

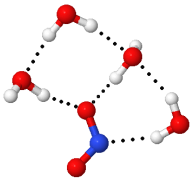

W_4S_{28}; ΔE_G=3.84
ΔE=0.60

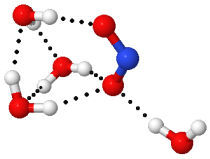

W_4S_{29}; ΔE_G=4.10
ΔE=0.62

W_3S_{30}; ΔE_G=4.17
ΔE=1.42

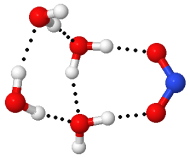

W_3S_{31}; ΔE_G=4.17
ΔE=0.42

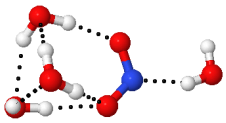

W_3S_{32}; ΔE_G=4.41
ΔE=1.35

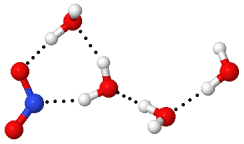

W_4S_{33}; ΔE_G=4.68
ΔE=3.23

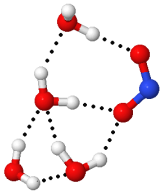

W_3S_{34}; ΔE_G=4.71
ΔE=1.44

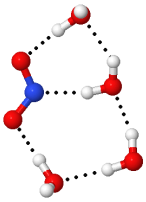

W_4S_{35}; ΔE_G=5.01
ΔE=1.33

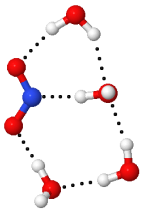

W_4S_{36}; ΔE_G=5.03
ΔE=1.42

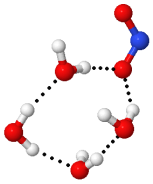

W_4S_{37}; ΔE_G=5.13
ΔE=2.39

W_4S_{38}; ΔE_G=5.16
ΔE=3.61

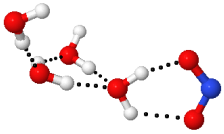

W_4S_{39}; ΔE_G=5.17
ΔE=3.49

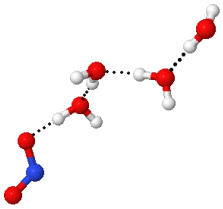

W_4S_{40}; ΔE_G=5.42
ΔE=6.18

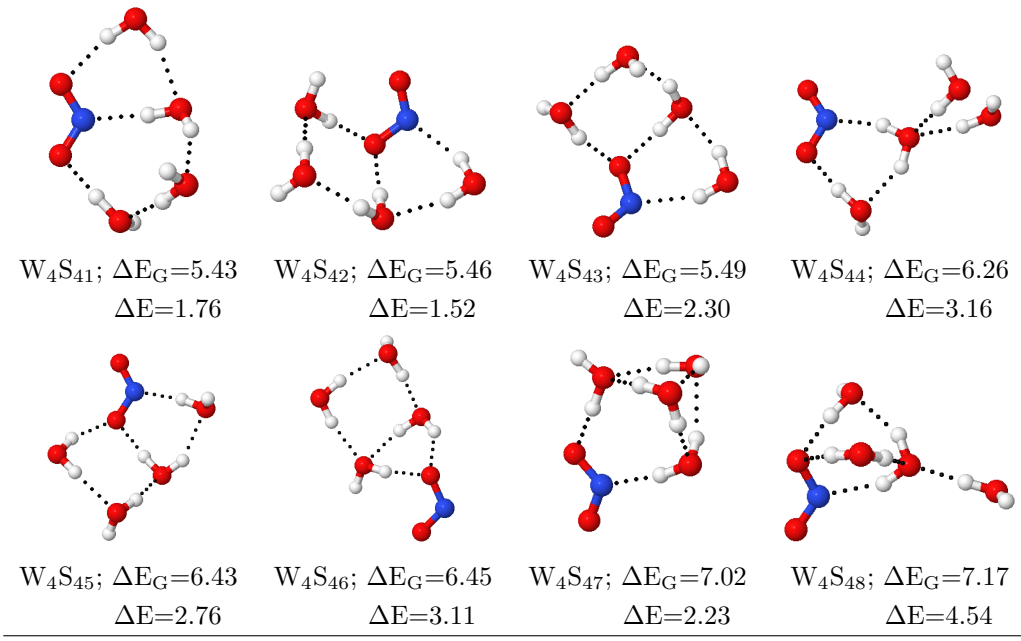

Figure S5: Structural motifs on the potential energy surface for $[NO_2(H_2O)_4]^-$. Dotted lines correspond to intermolecular contacts, those for which AIM predicts bonding paths. Data taken from the B3LYP/6-311++G(d,p) optimized geometries.

5.5 $x = 5$

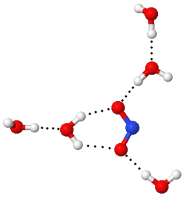

W_5S_1; ΔE_G=0.00
ΔE=2.39

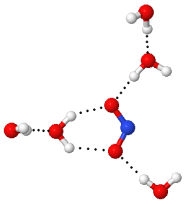

W_5S_2; ΔE_G=0.02
ΔE=2.25

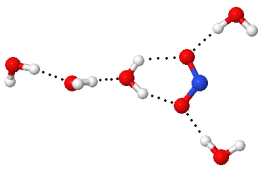

W_5S_3; ΔE_G=0.51
ΔE=2.58

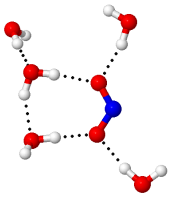

W_5S_4; ΔE_G=1.06
ΔE=1.92

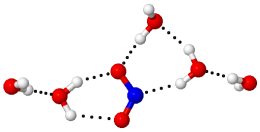

W_5S_5; ΔE_G=1.60
ΔE=1.51

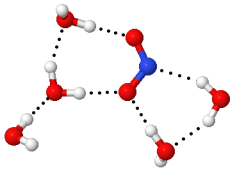

W_5S_6; ΔE_G=1.85
ΔE=1.25

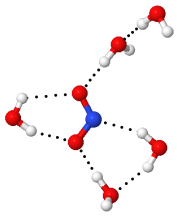

W_5S_7; ΔE_G=1.97
ΔE=2.67

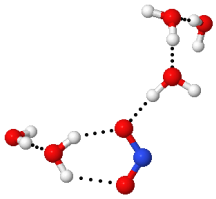

W_5S_8; ΔE_G=2.01
ΔE=3.38

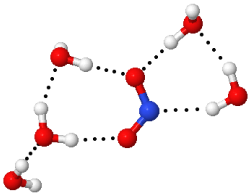

W_5S_9; ΔE_G=2.26
ΔE=1.08

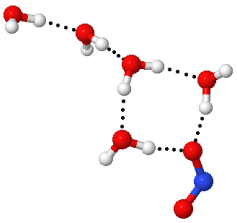

W_5S_{10}; ΔE_G=2.52
ΔE=2.38

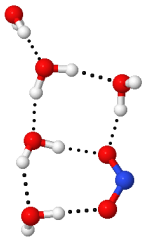

W_5S_{11}; ΔE_G=2.55
ΔE=1.04

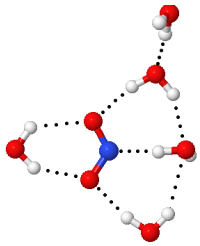

W_5S_{12}; ΔE_G=2.61
ΔE=2.31

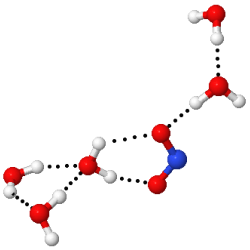

W_5S_{13}; ΔE_G=2.89
ΔE=3.19

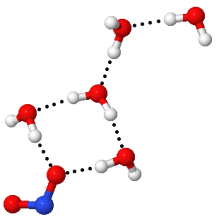

W_5S_{14}; ΔE_G=2.91
ΔE=2.40

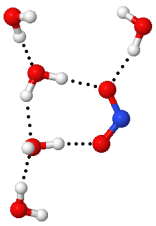

W_5S_{15}; ΔE_G=3.02
ΔE=3.53

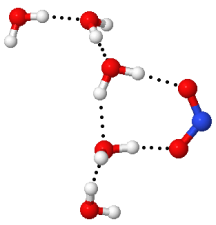

W_5S_{16}; ΔE_G=3.04
ΔE=3.92

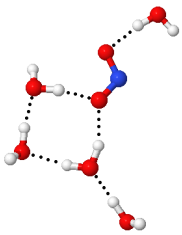

W_5S_{17}; ΔE_G=3.35
ΔE=2.59

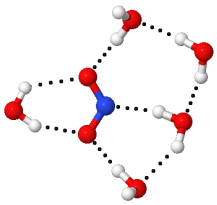

W_5S_{18}; ΔE_G=3.41
ΔE=1.46

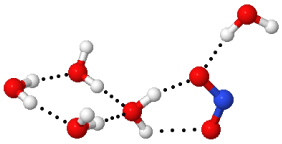

W_5S_{19}; ΔE_G=3.45
ΔE=2.49

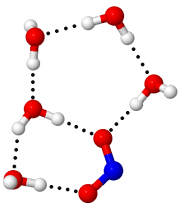

W_5S_{20}; ΔE_G=3.50
ΔE=0.94

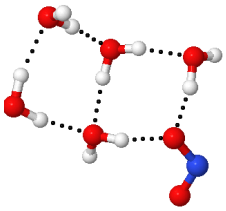

W_5S_{21}; ΔE_G=3.57
ΔE=2.47

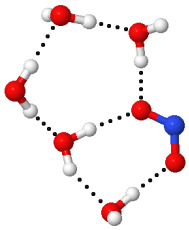

W_5S_{22}; ΔE_G=3.69
ΔE=1.73

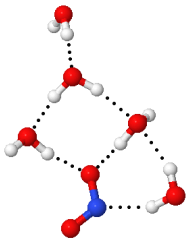

W_5S_{23}; ΔE_G=3.69
ΔE=1.92

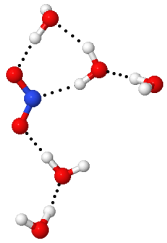

W_5S_{24}; ΔE_G=3.70
ΔE=3.83

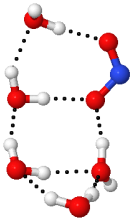

W_5S_{25}; ΔE_G=3.90
ΔE=1.91

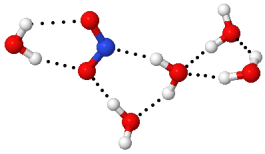

W_5S_{26}; ΔE_G=3.93
ΔE=2.47

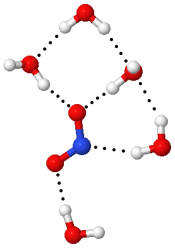

W_5S_{27}; ΔE_G=4.04
ΔE=2.87

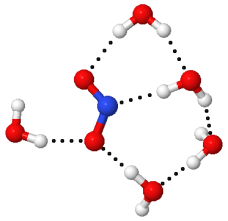

W_5S_{28}; ΔE_G=4.08
ΔE=2.07

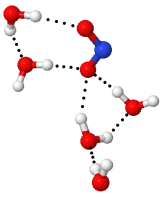

W_5S_{29}; ΔE_G=4.27
ΔE=4.05

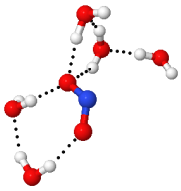

W_5S_{30}; ΔE_G=4.31
ΔE=1.32

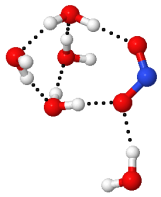

W_5S_{31}; ΔE_G=4.34
ΔE=2.02

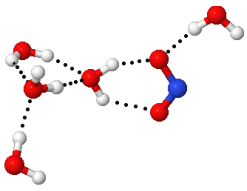

W_5S_{32}; ΔE_G=4.34
ΔE=4.65

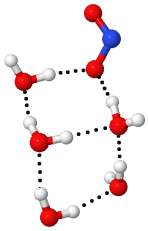

W_5S_{33}; ΔE_G=4.34
ΔE=1.91

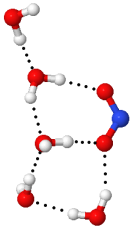

W_5S_{34}; ΔE_G=4.39
ΔE=2.82

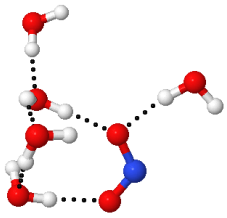

W_5S_{35}; ΔE_G=4.47
ΔE=2.91

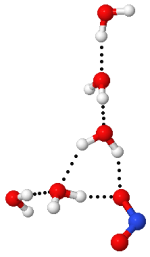

W_5S_{36}; ΔE_G=4.72
ΔE=5.85

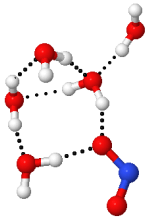

W_5S_{37}; ΔE_G=4.78
ΔE=3.61

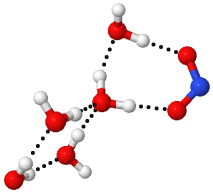

W_5S_{38}; ΔE_G=4.79
ΔE=2.68

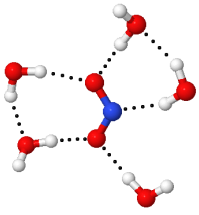

W_5S_{39}; ΔE_G=4.81
ΔE=2.87

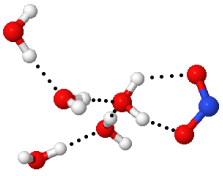

W_5S_{40}; ΔE_G=4.85
ΔE=6.51

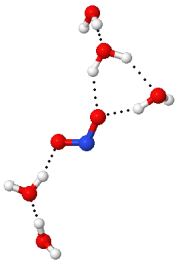

W_5S_{41}; ΔE_G=5.03
ΔE=5.39

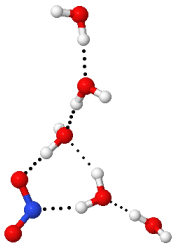

W_5S_{42}; ΔE_G=5.04
ΔE=5.50

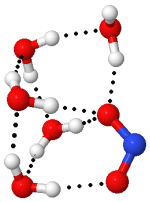

W_5S_{43}; ΔE_G=5.12
ΔE=0.00

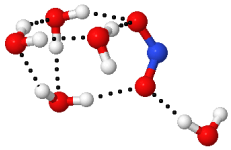

W_5S_{44}; ΔE_G=5.23
ΔE=1.87

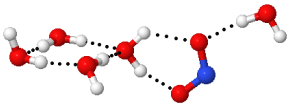

W_5S_{45}; ΔE_G=5.23
ΔE=3.78

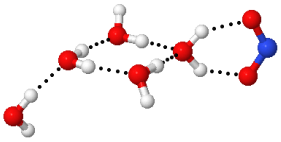

W_5S_{46}; ΔE_G=5.30
ΔE=3.95

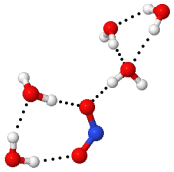

W_5S_{47}; ΔE_G=5.68
ΔE=4.20

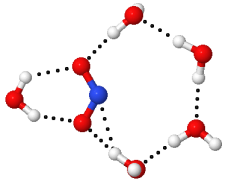

W_5S_{48}; ΔE_G=5.72
ΔE=14.72

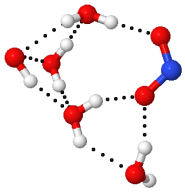

W_5S_{49}; ΔE_G=5.99
ΔE=2.70

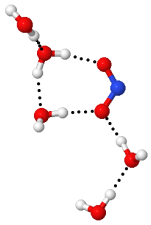

W_5S_{50}; ΔE_G=6.00
ΔE=3.83

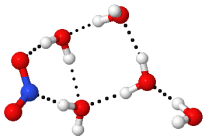

W_5S_{51}; ΔE_G=6.04
ΔE=3.70

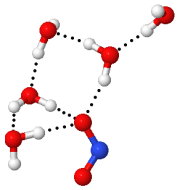

W_5S_{52}; ΔE_G=6.07
ΔE=4.00

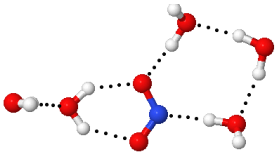

W_5S_{53}; ΔE_G=6.17
ΔE=3.10

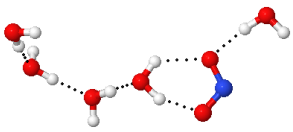

W_5S_{54}; ΔE_G=6.52
ΔE=5.49

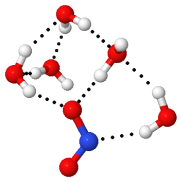

W_5S_{55}; ΔE_G=6.64
ΔE=3.46

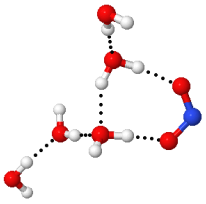

W_5S_{56}; ΔE_G=6.67
ΔE=5.00

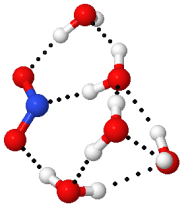

W_5S_{57}; ΔE_G=6.71
ΔE=2.04

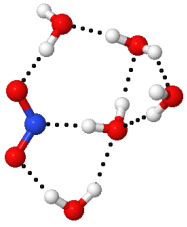

W_5S_{58}; ΔE_G=6.91
ΔE=3.38

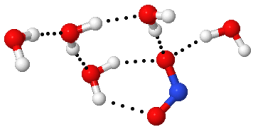

W_5S_{59}; ΔE_G=7.04
ΔE=5.54

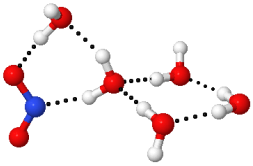

W_5S_{60}; ΔE_G=7.12
ΔE=4.45

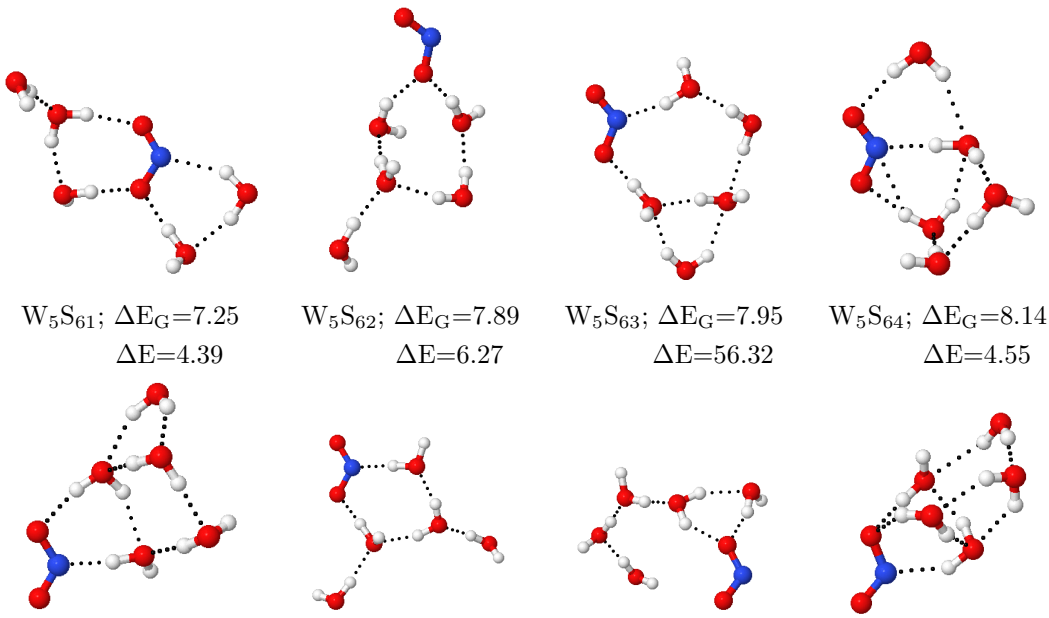

Figure S6: Structural motifs on the potential energy surface for $[NO_2(H_2O)_5]^-$. Dotted lines correspond to intermolecular contacts, those for which AIM predicts bonding paths. Data taken from the B3LYP/6-311++G(d,p) optimized geometries.

5.6 $x = 6$

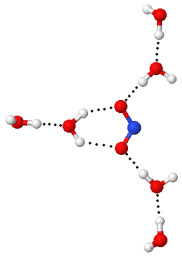

W_6S_1; ΔE_G=0.00
ΔE=3.82

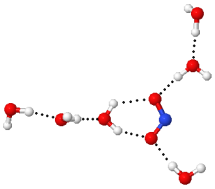

W_6S_2; ΔE_G=0.90
ΔE=3.97

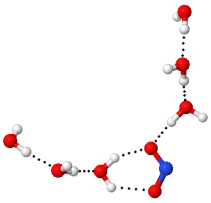

W_6S_3; ΔE_G=0.91
ΔE=4.47

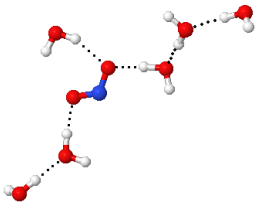

W_6S_4; ΔE_G=1.41
ΔE=4.65

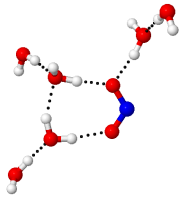

W_6S_5; ΔE_G=1.56
ΔE=4.17

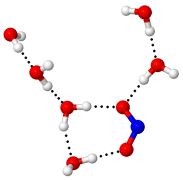

W_6S_6; ΔE_G=1.81
ΔE=3.51

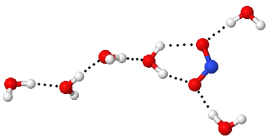

W_6S_7; ΔE_G=1.85
ΔE=4.69

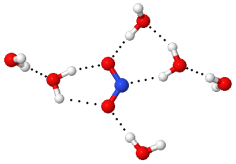

W_6S_8; ΔE_G=2.30
ΔE=3.12

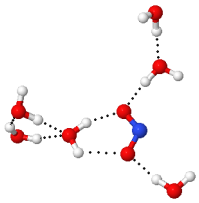

W_6S_9; ΔE_G=2.89
ΔE=4.23

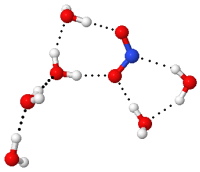

W_6S_{10}; ΔE_G=3.31
ΔE=2.72

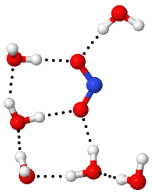

W_6S_{11}; ΔE_G=3.32
ΔE=2.06

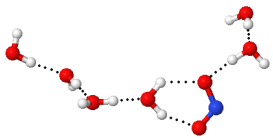

W_6S_{12}; ΔE_G=3.40
ΔE=5.28

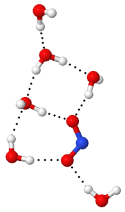

W_6S_{13}; ΔE_G=3.41
ΔE=2.58

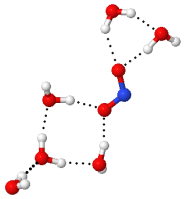

W_6S_{14}; ΔE_G=3.51
ΔE=3.58

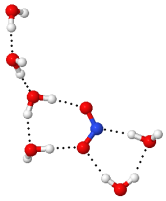

W_6S_{15}; ΔE_G=3.58
ΔE=3.05

W_6S_{16}; ΔE_G=3.87
ΔE=4.95

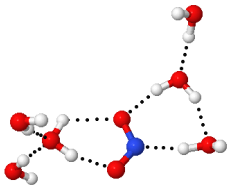

W_6S_{17}; ΔE_G=3.89
ΔE=4.57

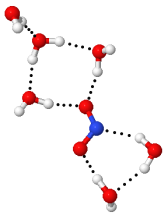

W_6S_{18}; ΔE_G=3.90
ΔE=2.61

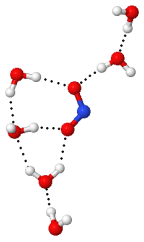

W_6S_{19}; ΔE_G=3.93
ΔE=4.89

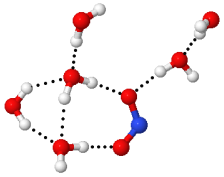

W_6S_{20}; ΔE_G=3.98
ΔE=4.36

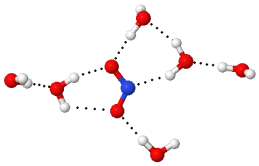

W_6S_{21}; ΔE_G=3.98
ΔE=3.45

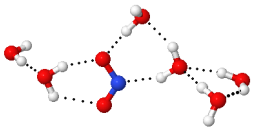

W_6S_{22}; ΔE_G=4.05
ΔE=3.23

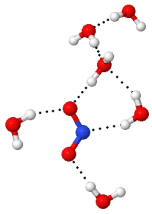

W_6S_{23}; ΔE_G=4.08
ΔE=4.94

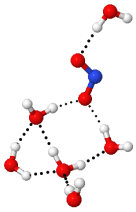

W_6S_{24}; ΔE_G=4.16
ΔE=3.43

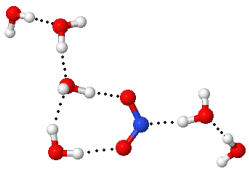

W_6S_{25}; ΔE_G=4.20
ΔE=6.15

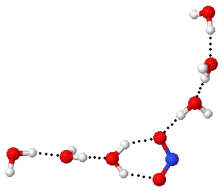

W_6S_{26}; ΔE_G=4.35
ΔE=5.12

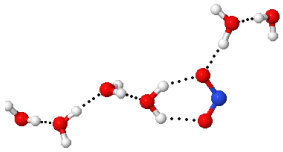

W_6S_{27}; ΔE_G=4.59
ΔE=5.73

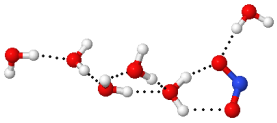

W_6S_{28}; ΔE_G=4.60
ΔE=5.61

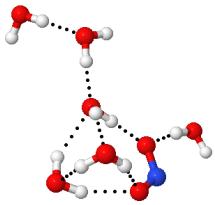

W_6S_{29}; ΔE_G=4.61
ΔE=4.11

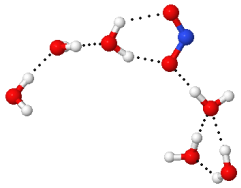

W_6S_{30}; ΔE_G=4.69
ΔE=5.38

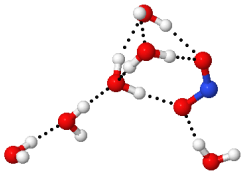

W_6S_{31}; ΔE_G=4.78
ΔE=4.14

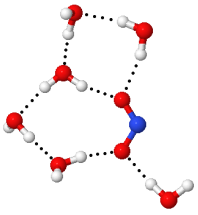

W_6S_{32}; ΔE_G=4.79
ΔE=3.15

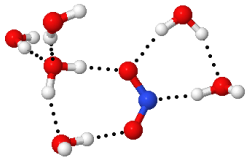

W_6S_{33}; ΔE_G=4.86
ΔE=4.41

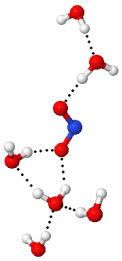

W_6S_{34}; ΔE_G=4.89
ΔE=6.42

W_6S_{35}; ΔE_G=4.96
ΔE=3.53

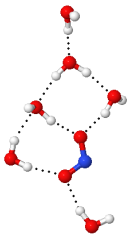

W_6S_{36}; ΔE_G=5.00
ΔE=2.90

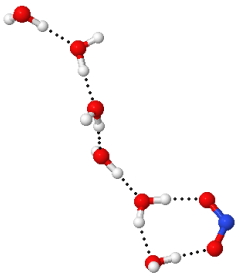

W_6S_{37}; ΔE_G=5.07
ΔE=6.66

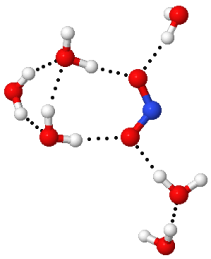

W_6S_{38}; ΔE_G=5.11
ΔE=4.49

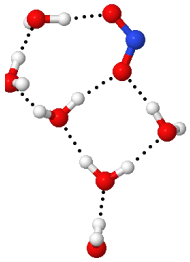

W_6S_{39}; ΔE_G=5.14
ΔE=2.31

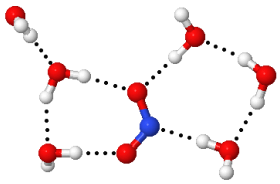

W_6S_{40}; ΔE_G=5.17
ΔE=3.14

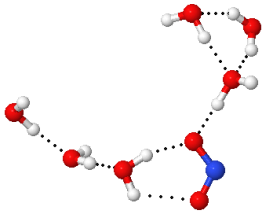

W_6S_{41}; ΔE_G=5.21
ΔE=5.22

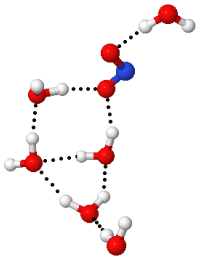

W_6S_{42}; ΔE_G=5.21
ΔE=4.20

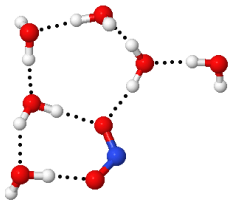

W_6S_{43}; ΔE_G=5.21
ΔE=2.88

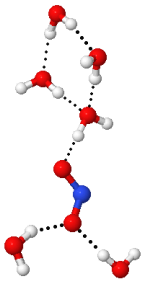

W_6S_{44}; ΔE_G=5.35
ΔE=5.75

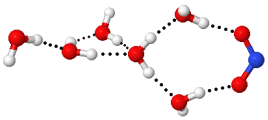

W_6S_{45}; ΔE_G=5.38
ΔE=4.58

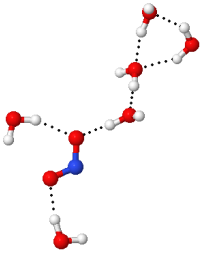

W_6S_{46}; ΔE_G=5.38
ΔE=6.67

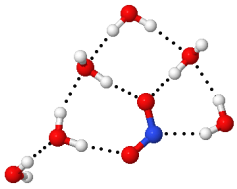

W_6S_{47}; ΔE_G=5.40
ΔE=2.93

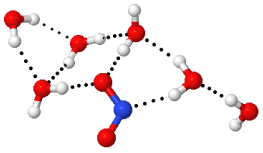

W_6S_{48}; ΔE_G=5.41
ΔE=3.13

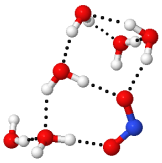

W_6S_{49}; ΔE_G=5.62
ΔE=3.59

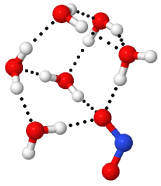

W_6S_{50}; ΔE_G=5.63
ΔE=0.00

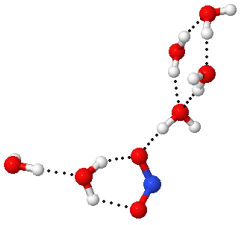

W_6S_{51}; ΔE_G=5.65
ΔE=4.82

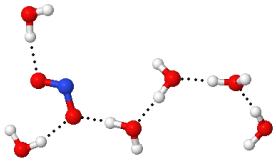

W_6S_{52}; ΔE_G=5.71
ΔE=6.50

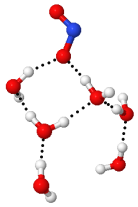

W_6S_{53}; ΔE_G=5.77
ΔE=6.18

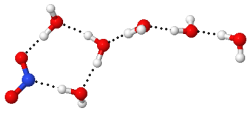

W_6S_{54}; ΔE_G=5.87
ΔE=5.81

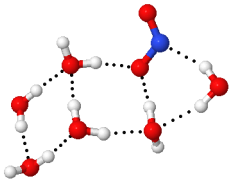

W_6S_{55}; ΔE_G=5.87
ΔE=2.30

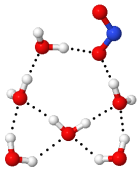

W_6S_{56}; ΔE_G=6.05
ΔE=4.17

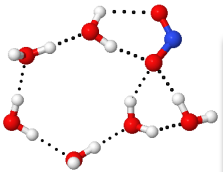

W_6S_{57}; ΔE_G=6.13
ΔE=4.26

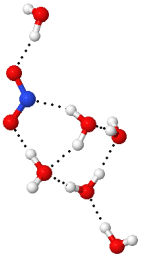

W_6S_{58}; ΔE_G=6.23
ΔE=4.51

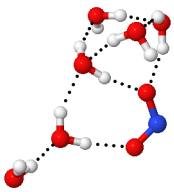

W_6S_{59}; ΔE_G=6.24
ΔE=3.20

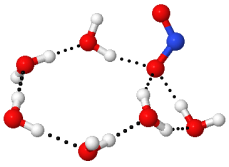

W_6S_{60}; ΔE_G=6.32
ΔE=4.23

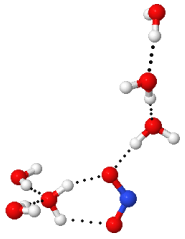

W_6S_{61}; ΔE_G=6.35
ΔE=6.14

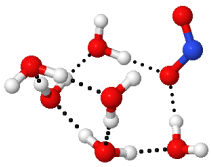

W_6S_{62}; ΔE_G=6.43
ΔE=2.59

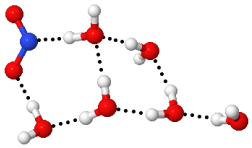

W_6S_{63}; ΔE_G=6.43
ΔE=4.07

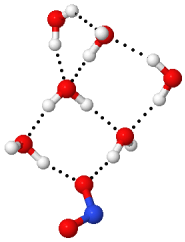

W_6S_{64}; ΔE_G=6.56
ΔE=3.45

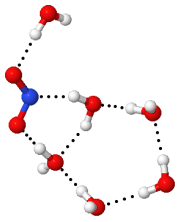

W_6S_{65}; ΔE_G=6.61
ΔE=4.60

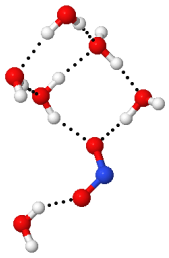

W_6S_{66}; ΔE_G=6.67
ΔE=5.25

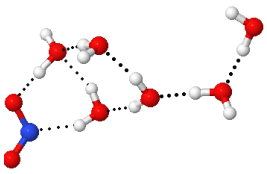

W_6S_{67}; ΔE_G=6.71
ΔE=4.96

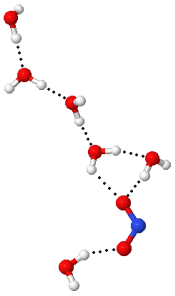

W_6S_{68}; ΔE_G=6.94
ΔE=9.24

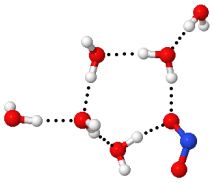

W_6S_{69}; ΔE_G=7.01
ΔE=6.89

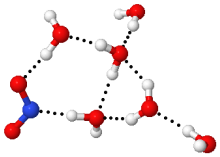

W_6S_{70}; ΔE_G=7.01
ΔE=5.77

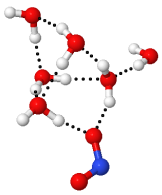

W_6S_{71}; ΔE_G=7.02
ΔE=3.73

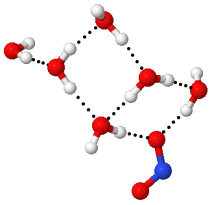

W_6S_{72}; ΔE_G=7.08
ΔE=2.69

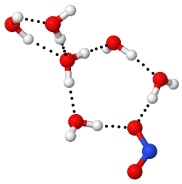

W_6S_{73}; ΔE_G=7.11
ΔE=4.00

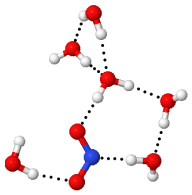

W_6S_{74}; ΔE_G=7.13
ΔE=4.34

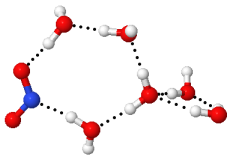

W_6S_{75}; ΔE_G=7.20
ΔE=5.30

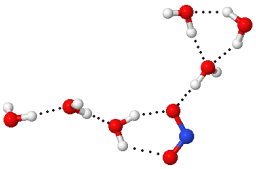

W_6S_{76}; ΔE_G=7.22
ΔE=5.82

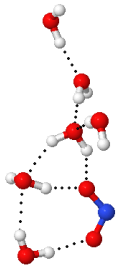

W_6S_{77}; ΔE_G=7.24
ΔE=7.61

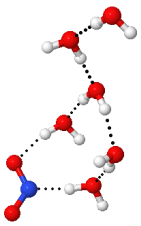

W_6S_{78}; ΔE_G=7.28
ΔE=5.87

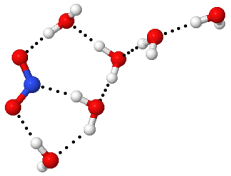

W_6S_{79}; ΔE_G=7.33
ΔE=4.23

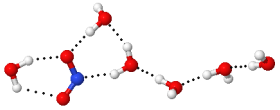

W_6S_{80}; ΔE_G=7.35
ΔE=5.33

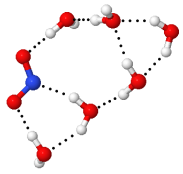

W_6S_{81}; ΔE_G=7.44
ΔE=3.75

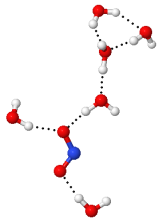

W_6S_{82}; ΔE_G=7.44
ΔE=8.41

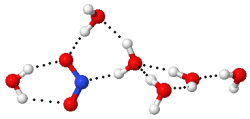

W_6S_{83}; ΔE_G=7.54
ΔE=4.86

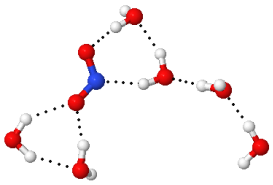

W_6S_{84}; ΔE_G=7.58
ΔE=6.05

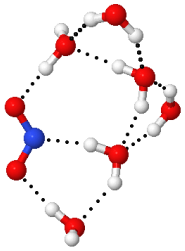

W_6S_{85}; ΔE_G=7.65
ΔE=3.59

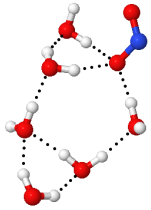

W_6S_{86}; ΔE_G=7.65
ΔE=4.28

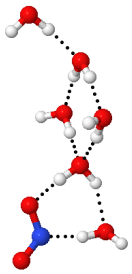

W_6S_{87}; ΔE_G=7.84
ΔE=4.96

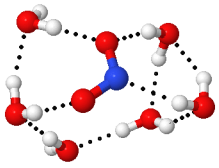

W_6S_{88}; ΔE_G=7.94
ΔE=2.42

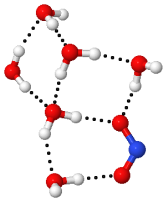

W_6S_{89}; ΔE_G=8.13
ΔE=2.69

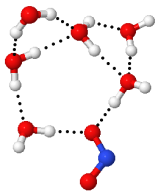

W_6S_{90}; ΔE_G=8.15
ΔE=5.32

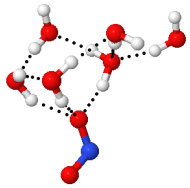

W_6S_{91}; ΔE_G=8.21
ΔE=5.02

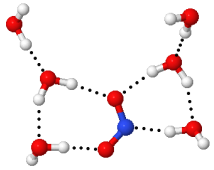

W_6S_{92}; ΔE_G=8.27
ΔE=4.68

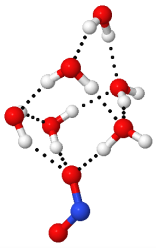

W_6S_{93}; ΔE_G=8.34
ΔE=3.39

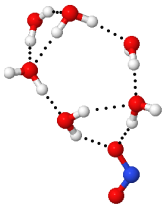

W_6S_{94}; ΔE_G=8.70
ΔE=6.33

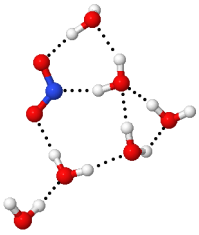

W_6S_{95}; ΔE_G=8.74
ΔE=5.57

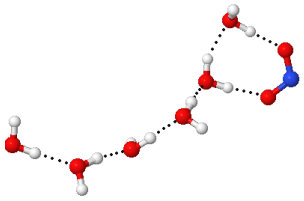

W_6S_{96}; ΔE_G=8.81
ΔE=8.22

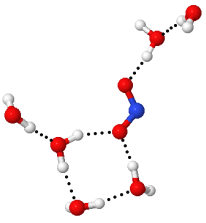

W_6S_{97}; ΔE_G=8.88
ΔE=6.89

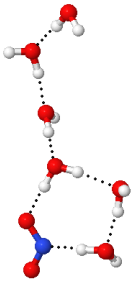

W_6S_{98}; ΔE_G=8.89
ΔE=7.44

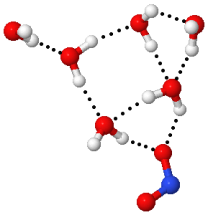

W_6S_{99}; ΔE_G=8.98
ΔE=7.14

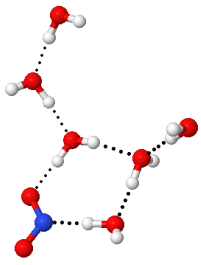

W_6S_{100}; ΔE_G=9.20
ΔE=8.78

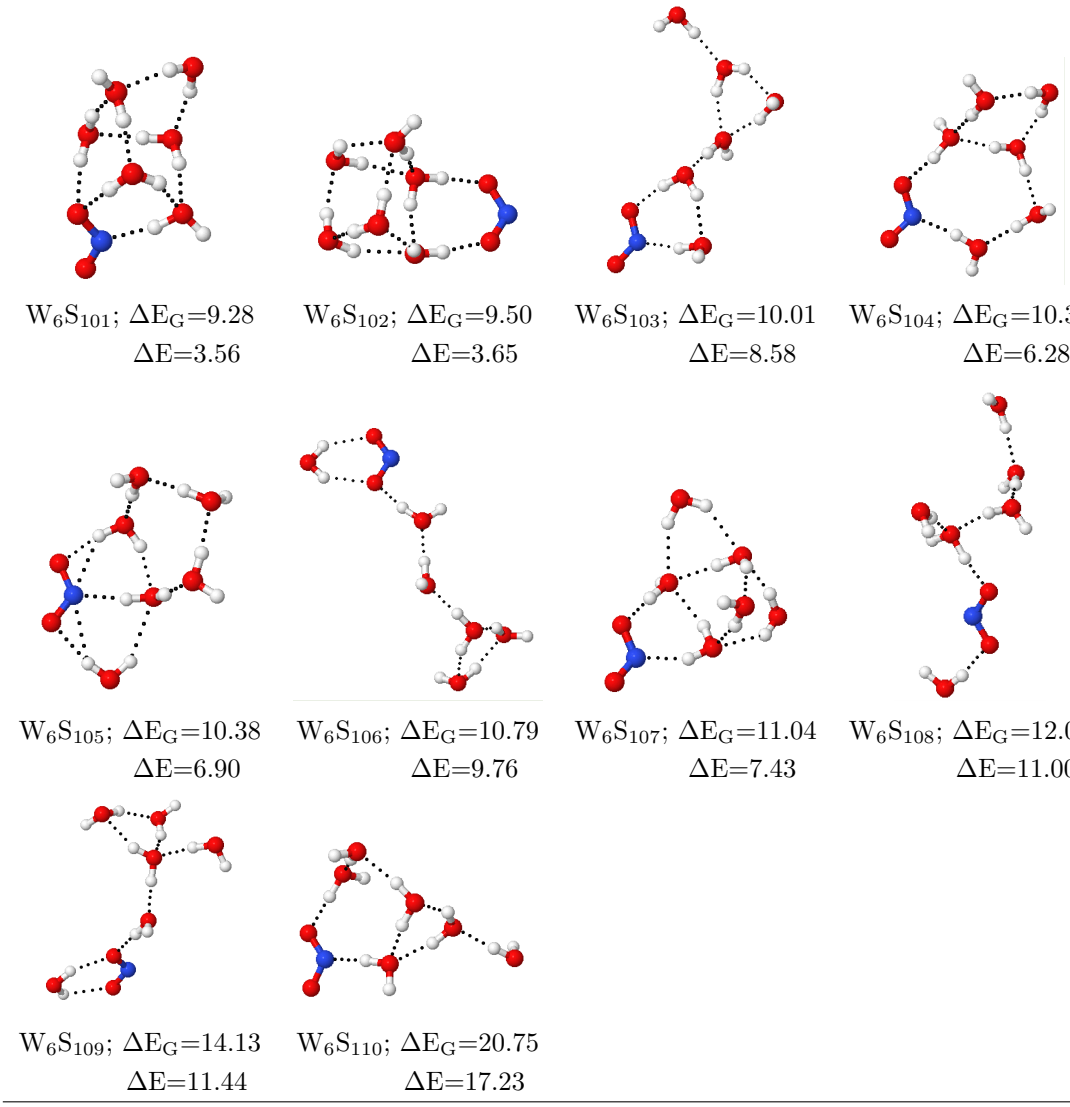

Figure S7: Structural motifs on the potential energy surface for $[NO_2(H_2O)_6]^-$. Dotted lines correspond to intermolecular contacts, those for which AIM predicts bonding paths. Data taken from the B3LYP/6-311++G(d,p) optimized geometries.

6 Vertical Excitation Energies in the QM/MM approaches

Table S4: Calculated spectral features for solvated NO_2^- using the B3LYP/6–311++G(d,p) model chemistry and two different charge models in the MD runs. Experimental $\lambda_{max} = 353.9$ (weak), $\lambda_{max} = 212.8$ nm (intense) as reported by Thomas and Brogat[10] for 10.6 and 3007 mg/L, respectively.

QM/MM approach	CM5 charges		RESP charges	
	$n \rightarrow \pi^*$	$\pi \rightarrow \pi^*$	$n \rightarrow \pi^*$	$\pi \rightarrow \pi^*$
QM/FQ (Rick)	336.13	179.86	337.27	180.51
QM/FQc	335.46	176.58	338.07	177.12
QM/FQc+rep	347.10	167.62	347.95	167.67
FQFμ	335.57	178.28	337.72	178.70
FQFμ+rep	347.22	169.00	347.71	169.03

7 CAM–B3LYP spectra

Table S5: Calculated spectral features for solvated NO_2^- using the CAM-B3LYP/6–311++G(d,p) model chemistry. Experimental $\lambda_{max} = 353.9$ (weak), $\lambda_{max} = 212.8$ nm (intense) as reported by Thomas and Brogat[10] for 10.6 and 3007 mg/L, respectively. x, the number water molecules in direct contact with NO_2^- is included

Sampling	Solvation model	x	CAM–B3LYP		mg NO_2^-/L sln
			$n \rightarrow \pi^*$ $\lambda_{max,1}$	$\pi \rightarrow \pi^*$ $\lambda_{max,2}$	
Isolated NO_2^-	PCM		364.03	190.51	
ASCEC	Gas phase cluster	1	370.49	242.45	
		2	365.59	220.95	
		3	363.14	221.70	
		4	355.78	206.11	
		5	353.95	203.00	
		6	353.99	184.01	
ASCEC	Cluster + PCM	1	372.33	205.35	2.54
		2	366.81	189.88	1.27
		3	365.59	189.19	0.85
		4	358.85	187.03	0.64
		5	355.78	186.78	0.51
		6	357.01	186.09	0.42

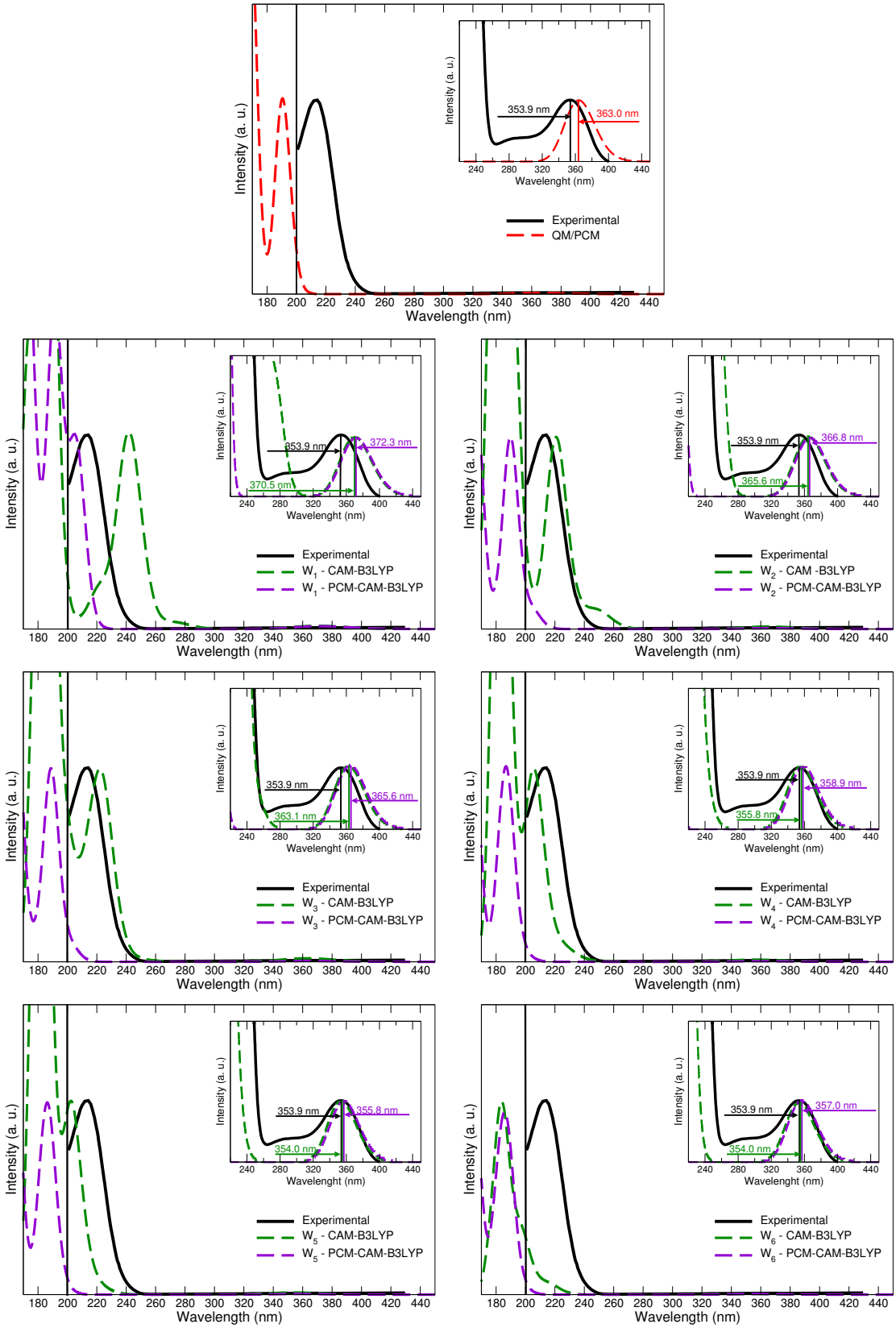

Figure S8: Experimental[10] (solid black line) and computed (dashed lines) spectra for aqueous nitrite at the CAM–B3LYP/6-311++G(d,p) level of theory. There is no experimental information to the left of the vertical solid lines. An inset showing the structure of the low intensity 353.9 nm band is also provided.

References

[1] M. J. Abrahama, T. Murtola, R. Schulz, S. Pálla, J. C. Smith, B. Hess, and E. Lindahl, "GROMACS: High performance molecular simulations through multi-level parallelism from laptops to supercomputers," *SoftwareX*, vol. 1-2, pp. 19–25, 2015.

[2] A. V. Marenich, S. V. Jerome, C. J. Cramer, and D. G. Truhlar, "Charge model 5: An extension of hirshfeld population analysis for the accurate description of molecular interactions in gaseous and condensed phases," *J. Chem. Theory Comput.*, vol. 8, no. 2, pp. 527–541, 2012. PMID: 26596602.

[3] C. I. Bayly, P. Cieplak, W. Cornell, and P. A. Kollman, "A well-behaved electrostatic potential based method using charge restraints for deriving atomic charges: the resp model," *The Journal of Physical Chemistry*, vol. 97, no. 40, pp. 10269–10280, 1993.

[4] J. Wang, R. M. Wolf, J. W. Caldwell, P. A. Kollman, and D. A. Case, "Development and testing of a general amber force field," *J. Comput. Chem.*, vol. 25, no. 9, pp. 1157–1174, 2004.

[5] P. Mark and L. Nilsson, "Structure and dynamics of the TIP3P, SPC, and SPC/E water models at 298 K," *J. Phys. Chem. A*, vol. 105, no. 43, pp. 9954–9960, 2001.

[6] G. Bussi, D. Donadio, and M. Parrinello, "Canonical sampling through velocity rescaling," *J. Chem. Phys.*, vol. 126, no. 1, p. 014101, 2007.

[7] M. Parrinello and A. Rahman, "Strain fluctuations and elastic constants," *J. Chem. Phys.*, vol. 76, no. 5, pp. 2662–2666, 1982.

[8] T. Darden, D. York, and L. Pedersen, "Particle mesh ewald: An nlog(n) method for ewald sums in large systems," *J. Chem. Phys.*, vol. 98, no. 12, pp. 10089–10092, 1993.

[9] H. J. Berendsen and W. F. Van Gunsteren, "Practical algorithms for dynamic simulations," *Molecular-dynamics simulation of statistical-mechanical systems*, pp. 43–65, 1986.

[10] O. Thomas and M. Brogat, "Chapter 12 - uv spectra library," in *UV-Visible Spectrophotometry of Water and Wastewater (Second Edition)* (O. Thomas and C. Burgess, eds.), pp. 379 – 517, Elsevier, second edition ed., 2017.